

Intelligent nanoflowers: A full tumor microenvironment-responsive multimodal cancer theranostic nanoplatform

Xunan Jing,^a Yanzi Xu,^a Daomeng Liu,^a Youshen Wu,^a Na Zhou,^a Daquan Wang,^a Kai Yan,^a

Lingjie Meng^{*ab}

^a School of Science, MOE Key Laboratory for Nonequilibrium Synthesis and Modulation of Condensed Matter, Xi'an Key Laboratory of Sustainable Energy Material Chemistry, Xi'an Jiaotong University, Xi'an 710049, P. R. China.

^b Instrumental Analysis Center of Xi'an Jiaotong University, Xi'an 710049, P. R. China.

* Corresponding author, Email: menglingjie@mail.xjtu.edu.cn



Fig. S1 TEM image of MnO₂ nanosheets without FHPC NPs.

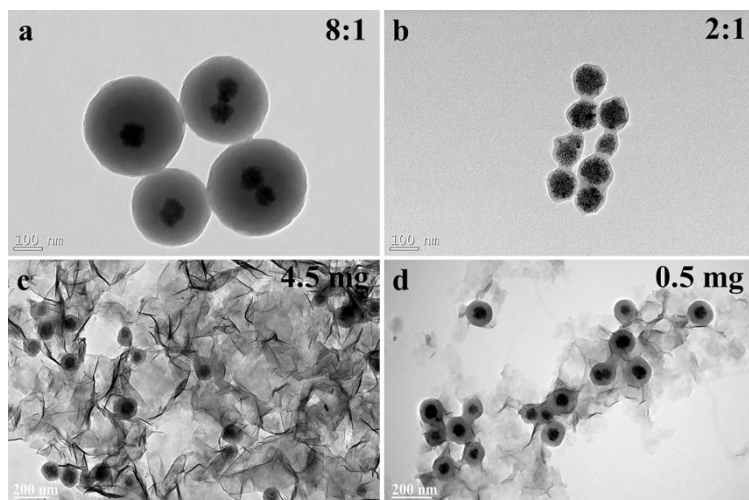


Fig. S2 (a-b) TEM images of FHCPC NPs (CUR to Ce6 molar ratios (8:1 and 2:1), respectively.); (c-d) TEM images of FHCPC@MnO₂ nanoflowers (KMnO₄ contents (4.5 mg and 0.5 mg), respectively.).

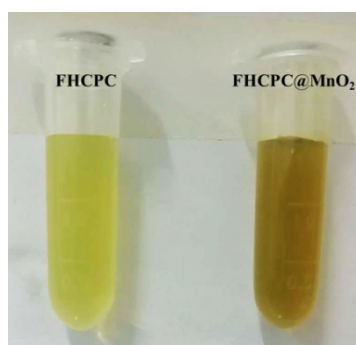


Fig. S3 Digital photo of FHCPC NPs (left) and FHCPC@MnO₂ nanoflowers (right) (25 $\mu\text{g mL}^{-1}$).

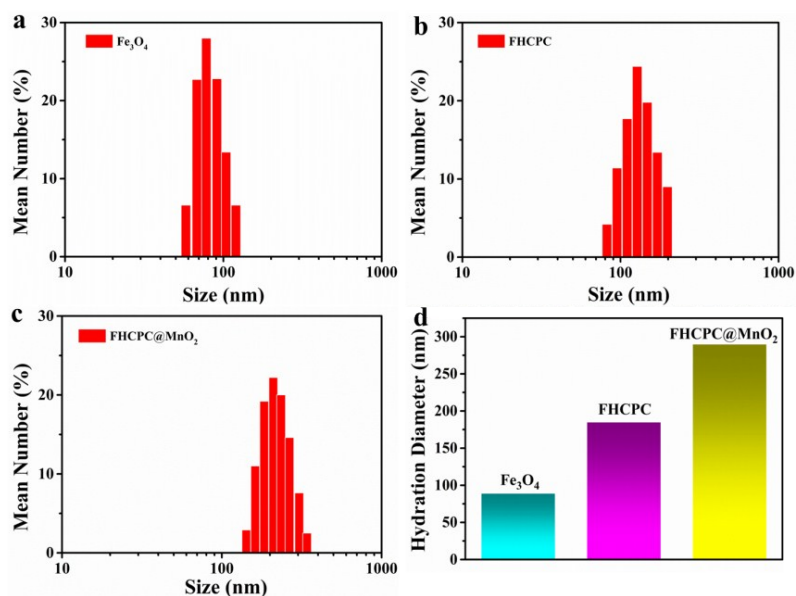


Fig. S4 Hydrodynamic diameters distribution of (a) Fe₃O₄ NCs; (b) FHCPC NPs; (c) and (d) FHCPC@MnO₂ nanoflowers and their average size statistics.

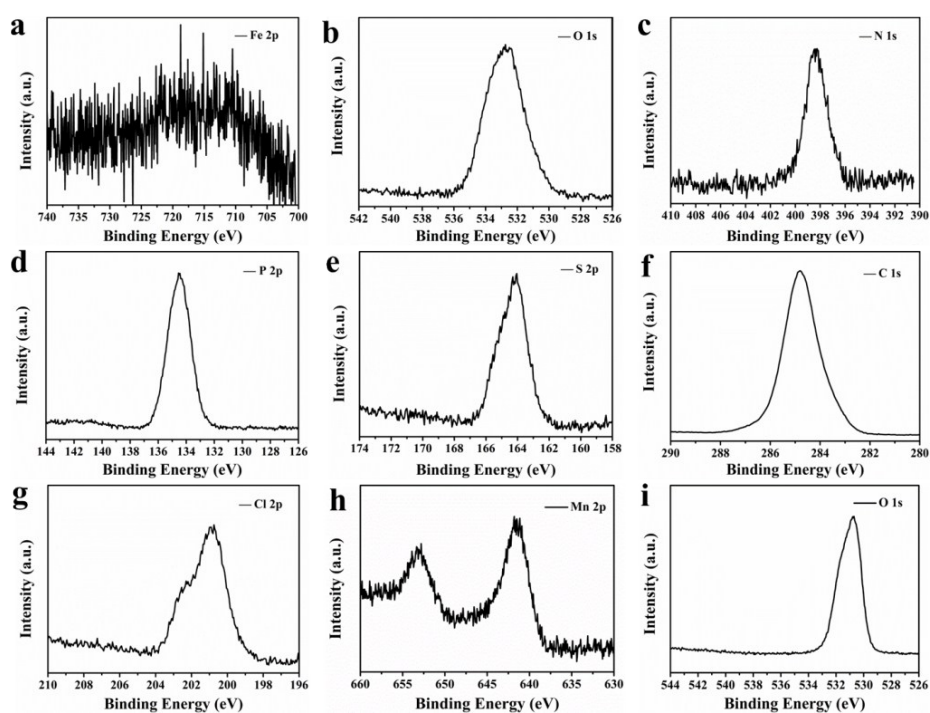


Fig. S5 XPS spectrum of FHCPC@MnO₂ nanoflowers: (a) Fe, (b) O, (c) N, (d) P, (e) S, (f) C, (g) Cl, (h) Mn and (i) O elements, together with their corresponding fitting curves.

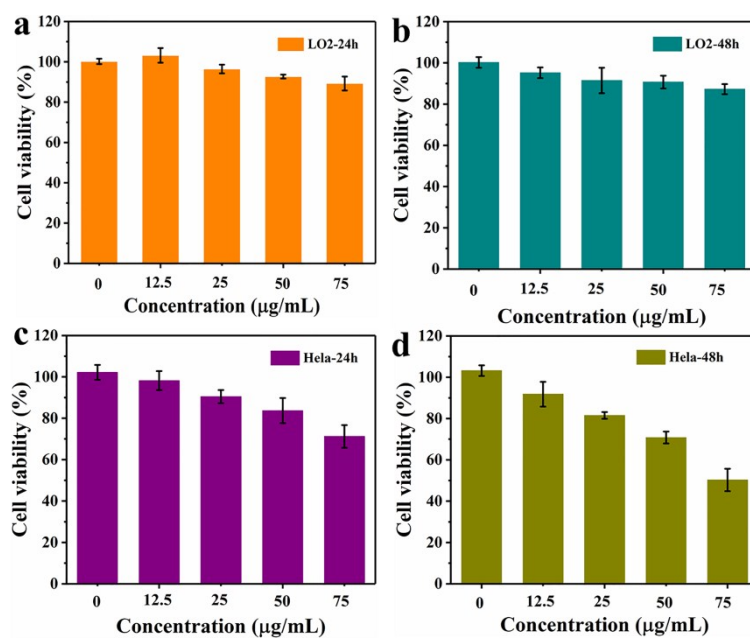


Fig. S6 (a, b) Cell viability of LO2 and (c, d) HeLa cells treated with various concentrations of FHCPC@MnO₂ nanoflowers for 24 and 48h in the dark, respectively.

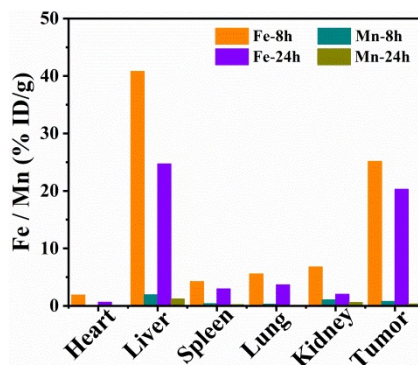


Fig. S7 Tissue distributions of Fe and Mn at time points of 8 and 24 h after intravenous injection of FHCPC@MnO₂ nanoflowers.

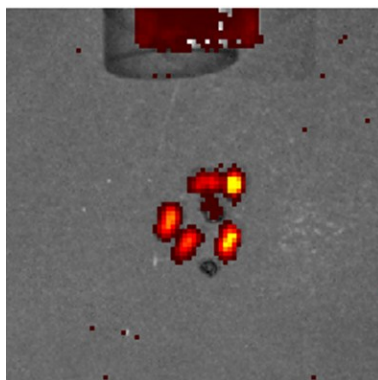


Fig. S8 Fluorescence image of tumor-bearing mice excreta at 8h after being treated with FHCPC@MnO₂ nanoflowers via intravenous injection.